Photonic crystals

Integration of a Close-Packed Quantum Dot Monolayer with a Photonic-Crystal Cavity Via Interfacial Self-Assembly and Transfer

Shisheng Xiong, Xiaoyu Miao, Jeffrey Spencer, Constantine Khripin, Ting S. Luk, and C. Jeffrey Brinker**

Nanoparticle (NP) assembly into ordered 2- and 3-D superlattices has stimulated enormous recent interest as a means to create new artificial solids whose electronic, magnetic, and optical behaviors can be tailored by the size dependent properties of the individual NPs mediated by coupling interactions with neighboring NPs,[1,2] suggesting applications in a diverse range of technologies including photovoltaics,[3] sensors,[4] catalysis,[5] and magnetic storage.[6] To date superlattice assembly has been demonstrated for monosized,[7] binary,[8] and even ternary systems,[9] allowing development and interrogation of a range of collective behaviors: electron transport within 2- and 3-D arrays of Coulomb islands,[10,11] Forster resonance energy transfer between superlattice monolayers in close proximity,[12] switchable optical properties through regulation of NP d-spacing,[1] and new magnetic behaviors based on binary superlattices.[13] Superlattice fabrication is performed principally by droplet evaporation[14] or convective assembly on an inclined plate.[15,16] These techniques are often slow, restricted in the size and topography of the substrate, and result in van der Waals solids with limited mechanical behaviors. To address these issues, we recently reported a general, rapid method to prepare large area, free-standing, NP/polymer monolayer superlattices by interfacial NP assembly within a polymer film on a water surface.[17] Although it is well known that the Langmuir-Blodgett technique has been used to produce well-controlled nanoparticle films,[18,19] our ultra-thin superlattices are highly robust and transferable to arbitrary substrates, owing to the polymer supporting layer.

Here we demonstrate interfacial self-assembly and transfer as an approach to address a long-standing technology challenge: how to integrate colloidal light emitters (e.g. semiconductor quantum dots) with a nanophotonic structure in a manner that achieves good quantum dot (QD) coupling with anti-nodes of the optical microcavity and avoids significant Q factor degradation. Enhancement of spontaneous emission from photo emitters coupled to the photonic crystal microcavity based on the Purcell effect[20] provides an ideal test for the integration of bottom-up self-assembly with top-down nanofabrication and means to study emitter behavior in microcavities. Standard spin-coating cannot achieve a high QD density, uniform film thickness, or controlled uniform separation between QDs over the photonic crystal surface.[21] Fabrication of a photonic crystal cavity around a single pre-screened Stranski-Krastanow grown QD with the desired optical properties is laborious, although exquisite control in position and wavelength is possible.[22] Templated growth of single quantum dots on GaAs (111)B surfaces has been demonstrated to provide good spatial control,[23] but suffers from low QD density and the requirement for precise control of the emission wavelength for high Q cavity applications.

Interfacial self-assembly (**Figure 1**a) provides a facile, rapid, scalable approach to assemble and transfer a large area NP array uniformly to a topographically complex photonic crystal surface (**Figure 2**). The transferred ultra-thin close-packed QD monolayer provides high density, uniformity and robustness, and controllable film thickness.[17] A seamless conformal interface between the QD monolayer and the photonic crystal microcavity is realized by either a 'picking' or 'lifting' transfer procedure (see Figure 1b and c). This allows optimal coupling between QDs and the photonic-crystal cavity, while relaxing the requirement of positioning individual QDs. Tuning the cavity resonance to the dot emission becomes unnecessary because the QD has a broad emission bandwidth. The uniformity and close proximity of the NP monolayer to the photonic crystal (Figure 2b, c) surface allows us to demonstrate an enhanced spontaneous emission of infrared quantum dots coupled to the defect cavity, while maintaining high Q.

S. Xiong, C. Khripin, Prof. C. J. Brinker
Department of Chemical and Nuclear Engineering
University of New Mexico
Albuquerque, NM 87106, USA
E-mail: cjbrink@sandia.gov
X. Miao, Dr. T. S. Luk, Prof. C. J. Brinker
Sandia National Laboratories
P.O. Box 5800, Albuquerque, NM 87185, USA
E-mail: tsluk@sandia.gov
X. Miao, Dr. T. S. Luk
Center for Integrated Nanotechnologies
Sandia National Laboratories
P.O. Box 5800, Albuquerque, NM 87185, USA
J. Spencer
Department of Mechanical Engineering
University of New Mexico
Albuquerque, NM 87106, USA

DOI: 10.1002/smll.201000897

© 2010 Wiley-VCH Verlag GmbH & Co. KGaA, Weinheim

small NANO MICRO

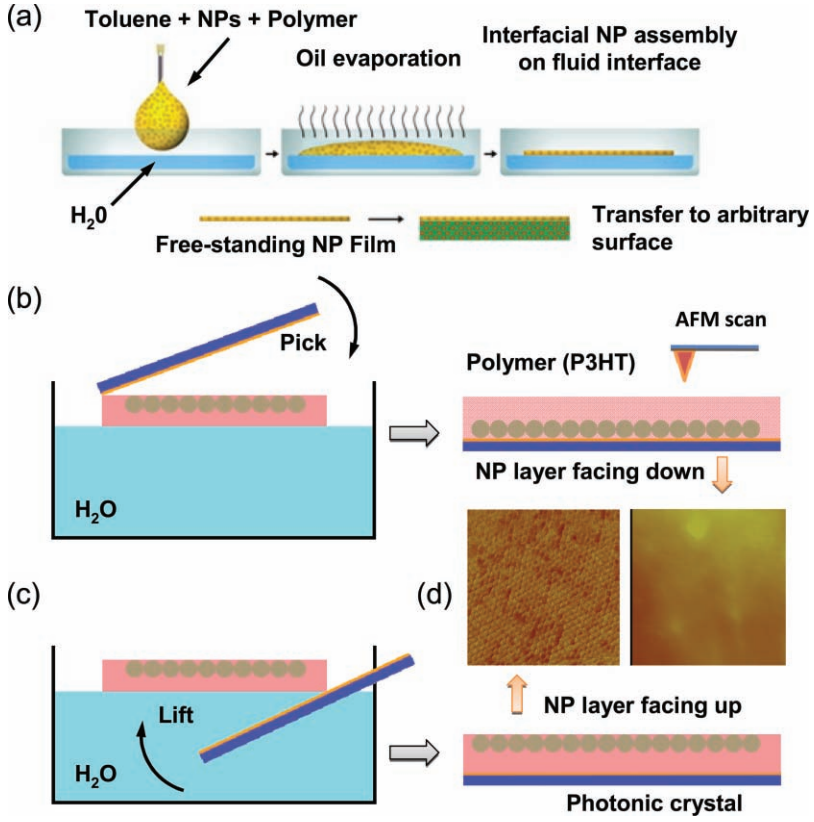

Figure 1. a) Schematic of the evaporation induced interfacial assembly and transfer process. b) Film transfer to the photonic crystal cavity by picking process results in a monolayer where the QDs are in close contact with the photonic crystal surface. c) For lifting, the QDs are about 20~50-nm away from the photonic crystal in the vertical direction. The AFM images (d) show the surface topography for the original vapor-side interface (AFM image of lifted monolayer) and for the original water-side interface. The dimension of the scanned image is 250 × 250 nm.

Self-assembly of the close-packed PbS QD/polymer monolayer was based on the interfacial evaporation induced self-assembly (EISA) procedure we recently reported,[17] and which we summarize briefly here. Oleic acid ligated PbS QDs (purchased from Evident Technologies) were dissolved in toluene containing polythiophene (P3HT) (interfacial assembly can be performed with many different polymers; P3HT is a representative example). One drop (about 8 µl) of the QD/P3HT/toluene solution was dispensed quickly by a syringe onto the surface of deionized water contained in a Petri dish. The droplet immediately spread into a film of ca. 5 cm diameter on the water surface. Solvent evaporation drives QD self-assembly followed by solidification within P3HT, the water interface maintaining the required QD mobility needed to achieve a highly ordered low defect QD monolayer. The resulting monolayer film is only 20 ~ 50 nm thick as determined by ellipsometry. The film thickness can be controlled by the polymer concentration in the solution (0.5–5 mg/ml in the case of P3HT). The hydrophobic PbS QDs reside preferentially at the air/polymer interface as determined by X-ray reflectivity measurements[24] and atomic force microscopy (AFM, see below). To transfer the monolayer to a photonic crystal or other device, we use the 'picking' or 'lifting' transfer procedures, respectively. As shown in Figure 1b, the picking process consists of lowering the photonic crystal device (see supporting information for fabrication process of the photonic crystal device; SEM images shown in Figure 2a, b.) from the air side toward the floating monolayer with the functional surface of the photonic crystal face down as illustrated in Figure 1b. This enables the QDs to be in close contact with the photonic crystal cavity, since the QDs reside at the polymer/air interface of the interfacially assembled array. In this case, the QDs and the photonic crystal are separated by only the stabilizing oleic acid ligand. To remove any residual water that might have been trapped in the film, the device was annealed at 100 °C for 5 minutes in air. For plasmonic applications where it is desirable to have a dielectric spacer between the QDs and the device surface in order to reduce the non-radiative damping,[25] the 'lifting' technique is more suitable. In this case, the photonic crystal substrate is first lowered into the water without touching the floating film, and then the substrate is retracted capturing the floating film with the polymer side down (Figure 1c).). The proximity of the QDs to the original vapor or water interfaces of the interfacially assembled monolayer is evident from AFM images of films transferred to silicon substrates by lifting or picking (Figure 1d). We observe an ordered nanoparticle surface topography for the original vapor side interface (AFM image of lifted monolayer) and a featureless topography for the original water interface (AFM image of picked monolayer). Here AFM is of course probing the opposite side of the film topography in contact with the photonic crystal surface for both transfer procedures.

We have obtained high quality PbS monolayer arrays using both P3HT and polystyrene polymers. It is important to note that, in both procedures the QD monolayer film remains freely suspended over the photonic-crystal surface without deforming and adhering to the side walls of the cavity. For example, Figure 2d shows a free-standing film suspended over a corner feature of the device. This is because the transferred QD/polymer film formed by this evaporation-induced interfacial assembly method is adherent and has a high elastic modulus. To directly measure the mechanical properties of the nanoparticle/polymer composite film, the monolayer array was transferred to a copper substrate with a single 150 µm diameter circular hole in the center via the lifting process. The deflections of the film under different AFM nano-indentation forces are shown in Figure S2. The Young's modulus of the PbS-P3HT film was determined to be about $10^{[9]}$ Pa using a simplified Reissner analysis.[26] To confirm that the quantum dots are indeed in a close-packed configuration, the film can be transferred to a TEM grid and examined as shown in Figure 2c. The density of

© 2010 Wiley-VCH Verlag GmbH & Co. KGaA, Weinheim

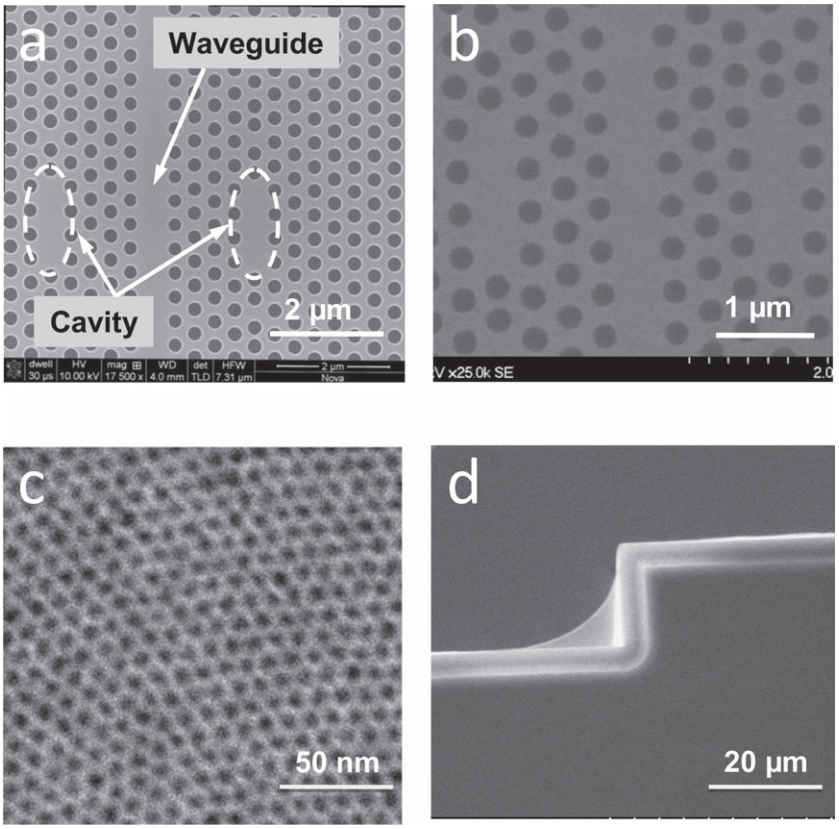

Figure 2. a,b) SEM images of a photonic crystal device before (a) and after (b) coating with a PbS-P3HT composite monolayer film. c) TEM image of the PbS-P3HT monolayer. d) a SEM image of a freely suspended monolayer spanning a corner feature of the device (This freely suspended region is used as a control to monitor optical properties of the monolayer itself).

the PbS QD in our sample is estimated from the TEM image to be about 2×10^{12} cm^{-2} with film non-uniformity less than 20%. As determined by GISAXS[24] interfacial assembly and transfer procedure allows us to achieve an ordered (uniform) close-packed QD array over large areas.

To demonstrate the importance of having the QD array in close contact with the photonic crystal cavity, we compared the enhanced photoluminescence (see supporting information for details of the optical characterization setup) from samples prepared by the 'picking' and 'lifting' transfer processes. **Figure 3**a shows a dramatic enhancement in photoluminescence from the cavity mode for the QD film transferred to the photonic crystal by picking (blue curve) versus the supported QD film transferred by lifting (red curve). The difference between the two photoluminescence measurements is consistent with the fact that the 'picking' process allows the QDs to be in close contact with the photonic-crystal cavity, providing better coupling to the cavity and thereby yielding a larger enhancement. In contrast, for the 'lifting' process, the coupling is dramatically reduced despite the QDs being separated by only 20–50 nm from the cavity in the vertical direction. In both samples, resonances are observed at about 1460 nm with the electric field polarized parallel to the waveguide axis. The broad background from the photoluminescence of QDs is similar to that obtained from a free-standing QD-polymer film (Figure 2d). The enhancement factor from the 'picking' process is about 7 times larger than the 'lifting' process. This ratio is consistent with a typical field decay length of 50 nm[27] and a typical film thickness of 50 nm. The emission lifetime of the 'picking' sample should be shorter than the 'lifting' sample. In these experiments, we made no attempt to use more mono-dispersed quantum dots than those commercially available. We estimate on average there are 20 QDs per nm bandwidth residing on the antinodes of the microcavity. With such a small number of emitters in a monolayer film, radiative lifetime measurement is proved to be difficult because of low emission rate (1–3 μsec radiative lifetime) and lack of suffciently low noise photon counting detector in this wavelength region. The highest Q factor observed with this deposition technique is about 8060 as shown in Figure 3(b), where the polarization of the photoluminescence is perpendicular to the waveguide axis To the best of our knowledge, this is the highest Q factor ever achieved using colloidal QDs coupled to a photonic crystal microcavity. We believe this Q factor reflects the quality of the photonic crystal rather than the transferred film. Numerical simulations have shown that theoretically the cavity Q with this polymer film can be as high as 25,000.[28]

In order to ensure the enhanced emission is not due to amplified spontaneous emission, we also measured the power dependence of the resonance position and Q factor of the photonic crystal cavity (data not shown here). We use the the Q factor and the ratio between the peak and the off resonant background near the resonance as indicators of amplified spontaneous emission effect. Within the resolution of the measurements (0.15 nm), we have not observed increase in Q factor nor any significant change in the peak to background ratio; constant to within 20% over several orders of magnitude change in the laser power. The intensity dependent data (not shown here) of composite films using P3HT and polystyrene are virtually identical, indicating that there is no change in the emission behavior that might have caused by charge transfer in P3HT; this result is consistent with Noone et. al.[29] In addition, the resonance location is independent of excitation intensity which implies the heating from the excitation laser has no impact to our studies.

In summary, we present a new and robust approach to deposit a uniform, densely packed and highly ordered QD/polymer monolayer onto a high Q photonic crystal cavity. A Q factor higher than 8000 has been achieved, indicating the compatibility of this technique with high Q cavities. This approach will enable applications that require integration of active nano-photonic emitting materials with passive micro-photonic structures.

© 2010 Wiley-VCH Verlag GmbH & Co. KGaA, Weinheim

NANO MICRO small

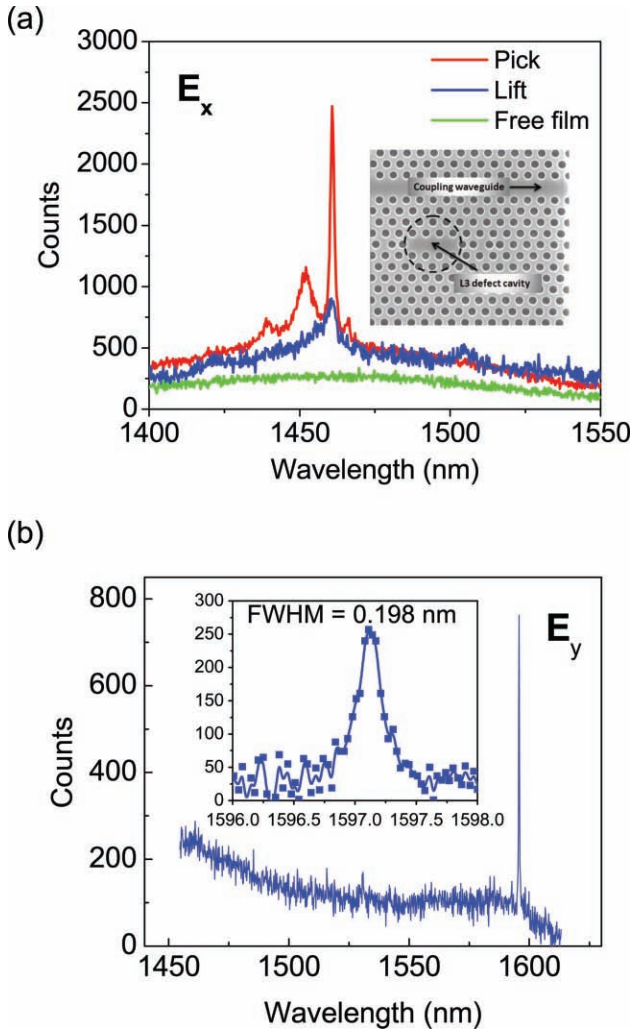

Figure 3. a) Comparison of PL signals from the QD-photonic crystal cavity systems prepared by picking or lifting transfer processes. The inset denotes the region of excitation marked by a black dashed circle. This resonance is referred to as E_x resonance with its emission polarization parallel to the waveguide. Also shown is the PL from a free-standing monolayer PbS-P3HT film. The PL is collected by a spectrometer with a 300 g/mm grating and 50 µm slit width. b) Enhanced photoluminescence spectrum of E_y resonance of an L3 photonic crystal microcavity collected by a spectrometer with a 300 g/mm grating and 50 µm slit width. The polymer used in the sample for this experiment is polystyrene. The inset shows a high-resolution measurement of the same resonance measured with a 900 g/mm grating and a 10 µm slit width. This resonance inherently has a much higher Q factor. The linewidth of the resonance is measured to be 0.198 nm and the corresponding Q factor is 8060.

Acknowledgements

This work is funded by the LDRD program of the Sandia National Laboratories and U.S. Department of Energy Office of Basic Energy Sciences NSET grant DE-FG02–02-ER15368 and the Office of Basic Energy Sciences Division of Materials Sciences and Engineering. Part of the work is performed at the Center for Integrated Nanotechnologies, a U.S. Department of Energy, Office of Basic Energy Sciences user facility. Sandia National Laboratories is a multi-program laboratory operated by Sandia Corporation, a Lockheed-Martin Company, for the U.S. Department of Energy under Contract No. DE-AC04–94AL85000.

[1] C. P. Collier, R. J. Saykally, J. J. Shiang, S. E. Henrichs, J. R. Heath, *Science* **1997**, *277*, 1978–1981.
[2] M. P. Pileni, *Abstracts of Papers of the American Chemical Society* **2001**, *222*, U218–U218.
[3] B. Oregan, M. Gratzel, *Nature* **1991**, *353*, 737–740.
[4] C. Y. Jiang, S. Markutsya, Y. Pikus, V. V. Tsukruk, *Nature Materials* **2004**, *3*, 721–728.
[5] M. Haruta, *Gold Bulletin* **2004**, *37*, 27–36.
[6] S. H. Sun, C. B. Murray, D. Weller, L. Folks, A. Moser, *Science* **2000**, *287*, 1989–1992.
[7] T. P. Bigioni, X. M. Lin, T. T. Nguyen, E. I. Corwin, T. A. Witten, H. M. Jaeger, *Nature Materials* **2006**, *5*, 265–270.
[8] E. V. Shevchenko, D. V. Talapin, N. A. Kotov, S. O'Brien, C. B. Murray, *Nature* **2006**, *439*, 55–59.
[9] W. H. Evers, H. Friedrich, L. Filion, M. Dijkstra, D. Vanmaekelbergh, *Angewandte Chemie-International Edition* **2009**, *48*, 9655–9657.
[10] T. B. Tran, I. S. Beloborodov, J. S. Hu, X. M. Lin, T. F. Rosenbaum, H. M. Jaeger, *Physical Review B* **2008**, *78*.
[11] H. Y. Fan, K. Yang, D. M. Boye, T. Sigmon, K. J. Malloy, H. F. Xu, G. P. Lopez, C. J. Brinker, *Science* **2004**, *304*, 567–571.
[12] M. Achermann, M. A. Petruska, S. A. Crooker, V. I. Klimov, *Journal of Physical Chemistry B* **2003**, *107*, 13782–13787.
[13] E. V. Shevchenko, D. V. Talapin, C. B. Murray, S. O'Brien, *Journal of the American Chemical Society* **2006**, *128*, 3620–3637.
[14] X. M. Lin, H. M. Jaeger, C. M. Sorensen, K. J. Klabunde, *Journal of Physical Chemistry B* **2001**, *105*, 3353–3357.
[15] D. V. Talapin, E. V. Shevchenko, M. I. Bodnarchuk, X. C. Ye, J. Chen, C. B. Murray, *Nature* **2009**, *461*, 964–967.
[16] D. K. Smith, B. Goodfellow, D. M. Smilgies, B. A. Korgel, *Journal of the American Chemical Society* **2009**, *131*, 3281–3290.
[17] J. B. Pang, S. S. Xiong, F. Jaeckel, Z. C. Sun, D. Dunphy, C. J. Brinker, *Journal of the American Chemical Society* **2008**, *130*, 3284-+.
[18] V. Santhanam, J. Liu, R. Agarwal, R. P. Andres, *Langmuir* **2003**, *19*, 7881–7887.
[19] A. P. Kulkarni, K. M. Noone, K. Munechika, S. R. Guyer, D. S. Ginger, *Nano Letters* **2010**, *10*, 1501–1505.
[20] E. M. Purcell, *Physical Review* **1946**, *69*.
[21] I. Fushman, D. Englund, J. Vuckovic, *Applied Physics Letters* **2005**, *87*.
[22] K. Hennessy, A. Badolato, M. Winger, D. Gerace, M. Atature, S. Gulde, S. Falt, E. L. Hu, A. Imamoglu, *Nature* **2007**, *445*, 896–899.
[23] A. Surrente, P. Gallo, M. Felici, B. Dwir, A. Rudra, E. Kapon, *Nanotechnology* **2009**, *20*, 415205.
[24] Shisheng Xiong, Darren Dunphy, Zhang Jiang, Jing Wang, C. J. Brinker, to be published.
[25] J. R. Lakowicz, K. Ray, M. Chowdhury, M. Szymanska, J. Zhang, K. Nowaczyk, *Analyst* **2008**, *133*.
[26] U. Komaragiri, M. R. Begley, J. G. Simmonds, *Trans. ASME, J. Appl. Mech.* **2005**, *72*, 203–212.
[27] J. T. Robinson, S. F. Preble, M. Lipson, *Optics Express* **2006**, *14*, 10588–10595.
[28] T. S. Luk, W. W. Chow, S. Xiong, X. Miao, B. G. Farfan, I. El-Kady, P. J. Resnick, M. F. Su, G. Subramania, M. R. Taha, C. J. Brinker, to be published.
[29] K. M. Noone, N. C. Anderson, N. E. Horwitz, A. M. Munro, A. P. Kulkarni, D. S. Ginger, *Acs Nano* **2009**, *3*, 1345–1352.
[30] Y. Akahane, T. Asano, B. S. Song, S. Noda, *Nature* **2003**, *425*.

Received: May 25, 2010
Revised: July 21, 2010
Published online: September 3, 2010

 © 2010 Wiley-VCH Verlag GmbH & Co. KGaA, Weinheim